

Magnetic-Field-Induced Superconductivity in Ultrathin Pb Films with Magnetic Impurities

Masato Niwata, Ryuichi Masutomi, and Tohru Okamoto

Department of Physics, University of Tokyo, 7-3-1 Hongo, Bunkyo-ku, Tokyo 113-0033, Japan

(Dated: October 23, 2017)

It is well known that external magnetic fields and magnetic moments of impurities both suppress superconductivity. Here, we demonstrate that their combined effect enhances the superconductivity of a few atomic layer thick Pb films grown on a cleaved GaAs(110) surface. A Ce-doped film, where superconductivity is totally suppressed at a zero field, actually turns superconducting when an external magnetic field is applied parallel to the conducting plane. For films with Mn adatoms, the screening of the magnetic moment by conduction electrons, i.e., the Kondo singlet formation, becomes important. We found that the degree of screening can be reduced by capping the Pb film with a Au layer, and observed the positive magnetic field dependence of the superconducting transition temperature.

In 1914, Kamerlingh Onnes reported the destructive effect of a magnetic field on the superconductivity of Pb and Sn [1]. Today, it is conventional wisdom that external magnetic fields, as well as magnetic impurities, break the time-reversal symmetry of Cooper pairs and tend to suppress superconductivity. There are two mechanisms responsible for this: the orbital effect (OE) and the paramagnetic effect (PE) [2, 3]. In the case of a superconductor containing magnetic elements, localized magnetic moments are also affected by the magnetic field. This should lead to an additional effect on superconductivity while it is usually obscured by OE and/or PE. For atomically thin or layered materials, OE can be eliminated by setting the magnetic field direction parallel to the conducting plane. Recently, it has been demonstrated that the reduction of the superconducting transition temperature T_c due to the parallel magnetic field H_{\parallel} is extremely small ($\sim 1\%$ for 10 T) in ultrathin Pb films grown on a cleaved GaAs(110) surface [4]. The suppression of PE was explained in terms of the spin precession due to the Rashba field [5, 6], which allows nonmagnetic scattering by defects to mix the spin-up state and spin-down state [7]. In this study, we employ ultrathin Pb films as the host superconductor to minimize OE and PE, which act directly on conduction electrons, and investigate the magnetic-field effect on superconductivity related to magnetic impurities. For films with Ce, we observe pronounced positive H_{\parallel} dependence of T_c . Furthermore, in a Pb-Ce(10 at%) alloy film, H_{\parallel} actually induces a quantum phase transition from the normal state to the superconducting state. These results are consistent with a recent theory by Kharitonov and Feigelman [8]. In the case of deposition of 3d transition metals, the exchange coupling is strong and the localized moment of an adatom is expected to be screened by conduction electrons, forming the Kondo singlet state [9]. We find that the exchange coupling is weakened on a Pb film covered with a Au layer and observe the positive H_{\parallel} dependence of T_c for Mn deposition.

The films were grown by vapor deposition onto a non-doped insulating GaAs single-crystal substrate, which

was cooled down to liquid helium temperatures to avoid grain formation and impurity segregation. In the case of pure Pb, superconductivity can be observed even in the monolayer regime due to an atomically flat surface of the cleaved GaAs substrate [4]. Current and voltage electrodes were prepared in advance by the deposition of gold films onto noncleaved surfaces [10, 11]. The cleavage of GaAs, the deposition of metals, and resistance measurements were performed *in situ* under ultrahigh vacuum conditions. Since the superconducting transition temperature T_c did not change when the film was left overnight, we believe that the base pressure was low enough and contamination effects were negligible. The amount deposited was measured with a quartz crystal microbalance and determined with an accuracy of about 5%. The four-probe resistance of the ultrathin film on a cleaved GaAs(110) surface ($4 \times 0.35 \text{ mm}^2$) was measured using the standard lock-in technique at 13.3 Hz. The magnetic-field direction with respect to the surface normal was precisely controlled using a rotatory stage on which the sample was mounted, together with a Hall generator, a RuO₂ resistance thermometer, and a heater. The sample stage can be cooled to 0.5 K via a silver foil linked to a pumped ³He refrigerator. All the data were taken when the temperature of the sample stage was kept constant so as to ensure thermal equilibrium between the sample and the thermometer. The magnetoresistance effect of the RuO₂ resistance thermometer was systematically calibrated against the vapor pressure of the liquid ³He or ⁴He for various temperatures [12]. After the correction, T_c can be determined with a relative accuracy of better than 0.2%.

First, we studied the superconducting transition of a Pb film with an average thickness of $d = 0.65 \text{ nm}$ for different amounts of Ce deposition. While T_c decreases monotonically with increasing Ce coverage [13], the suppression rate is small. Even for a coverage near one monolayer, T_c decreases only by 40% (from 3.2 to 1.9 K). To enhance the exchange coupling between the localized moment of Ce and conduction electrons, we prepared two

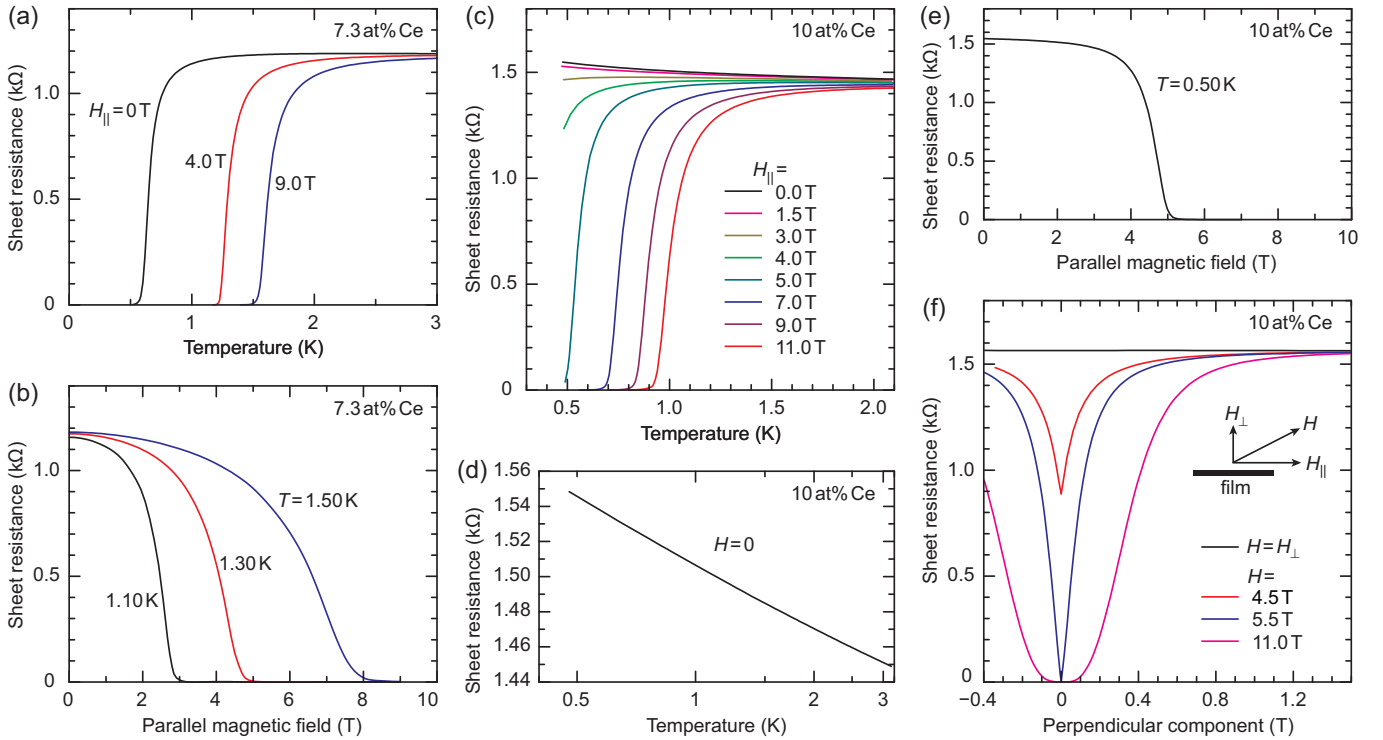


FIG. 1. Superconductivity of Pb-Ce alloy films enhanced or induced by parallel magnetic fields. (a) Sheet resistance R_{sq} of $F1$ (7.3 at% Ce) versus T for different H_{\parallel} . (b) H_{\parallel} dependence of R_{sq} of $F1$ at different temperatures. (c) R_{sq} of $F2$ (10.0 at% Ce) versus T for different H_{\parallel} . (d) Expanded plot of the zero-magnetic-field data in (c). (e) H_{\parallel} dependence of R_{sq} of $F2$ at $T = 0.50$ K. (f) H_{\perp} dependence of R_{sq} of $F2$ at $T = 0.50$ K for different values of $H = (H_{\perp}^2 + H_{\parallel}^2)^{1/2}$.

Pb-Ce alloy films ($F1$ and $F2$) where Ce atoms are expected to be dominantly surrounded by Pb atoms. They are 1.1 nm thick (approximately 3 atomic layers) and were formed from threefold alternate depositions of Ce and Pb. Figure 1(a) shows the T dependence of the sheet resistance R_{sq} of $F1$ (containing 7.3 at% Ce) for different values of H_{\parallel} . At zero magnetic field, superconductivity is strongly suppressed and R_{sq} becomes zero only below 0.6 K. With increasing H_{\parallel} , however, the superconducting transition obviously shifts to higher temperatures. In Fig. 1(b), R_{sq} is plotted as a function of H_{\parallel} for fixed temperatures at which the H_{\parallel} -induced resistance drop is clearly observed.

Figure 1(c) shows the T dependence of R_{sq} of $F2$ (containing 10 at% Ce) with varying H_{\parallel} . At zero magnetic field, $\partial R_{sq}/\partial T$ is negative and no superconducting behavior is observed down to 0.47 K [see also Fig. 1(d)]. This film becomes superconducting only in high parallel magnetic fields. In Fig. 1(e), the H_{\parallel} -induced resistance drop at $T = 0.50$ K is shown. In the presence of the perpendicular magnetic field component H_{\perp} , OE destroys the superconducting state. Figure 1(f) shows the H_{\perp} dependence of R_{sq} of $F2$ at $T = 0.50$ K obtained for different total strength H . For large H_{\perp} , R_{sq} approaches the normal-state value irrespective of H . The superconduct-

ing region around $H_{\perp} = 0$ becomes wider as H increases from 5.5 to 11 T, indicating the stabilization of superconductivity with respect to OE, as well as with respect to thermal fluctuations.

Magnetic-field-induced superconductivity has been observed before in several other materials [14–18]. Except for the special case of a spin-triplet superconductor URhGe [18], it was understood in terms of the Jaccarino-Peter (JP) mechanism [19], where PE of a mean field produced by aligned local magnetic moments through the antiferromagnetic exchange interaction is compensated by the external magnetic field. However, this mechanism is unlikely to account for our results. As described above, PE is strongly suppressed in ultrathin Pb films, for which the Pauli-limiting field is estimated to be on the order of 100 T. Furthermore, since the mean field is absent at zero magnetic field, where the magnetic moments are expected to be randomly oriented, the JP model does not explain why superconductivity is suppressed at $H = 0$.

The enhancement of T_c by H_{\parallel} in Pb films without intentional impurities was reported in Ref. [20]. The maximum enhancement reaches 13.5% at $H_{\parallel} = 8$ T for $d = 1.2$ nm. However, no theory adequately explains the positive H_{\parallel} dependence of T_c in pure Pb. For Pb films grown on a cleaved GaAs surface, we did not ob-

serve the enhancement of T_c by H_{\parallel} at least in the range $0.22 \leq d \leq 3.0$ nm unless magnetic impurities were added. This discrepancy might be due to the difference in substrates and film morphology.

According to the pioneering theory of Abrikosov and Gor'kov [21], the exchange scattering of electrons by magnetic impurities suppresses superconductivity. Recently, Kharitonov and Feigelman (KF) have shown that the pair-breaking effect is weakened by the polarization of impurities in a magnetic field [8]. While the polarization increases the rate of scattering without spin flip, it decreases the spin-flip scattering rate. The total exchange scattering rate is reduced from its zero-magnetic-field value ν_s to $\nu_s S/(S+1)$ as the magnetic field increases to infinity. Here, S is the spin of the impurity. It has been predicted that a magnetic field can induce a superconducting quantum phase transition when ν_s is in an appropriate range and PE is strongly reduced due to spin-orbit scattering. In ultrathin Pb films, high spin-orbit scattering rate is expected to be effectively achieved by the combination of the Rashba field and nonmagnetic scattering [7]. In Fig. 2(a), T_c in F1 and F2, which is defined as the temperature at which R_{sq} is half the normal-state value R_N , is plotted as a function of H_{\parallel} . Solid curves are the best fits based on the KF theory, assuming $S = 1/2$ for Ce and neglecting OE and PE. The calculation well reproduces the experimental results with only two fitting parameters, ν_s and T_{c0} (T_c in the absence of exchange scattering). The ratio $\hbar\nu_s/k_B T_{c0}$ exceeds a critical value of 0.882 [8] for F2, while it does

not for F1. The quantum phase transition is calculated to occur at $H_c = 2.7$ T. Near the critical point, T_c varies approximately as $(H_{\parallel} - H_c)^{1/2}$. To see this, T_c^2 is plotted for F2 in Fig. 2(b). The experimental data almost fall on a straight line, which cuts the H_{\parallel} -axis at H_c . According to the present calculation, T_c increases monotonically with H_{\parallel} and approaches a constant value. This is in contrast to the JP mechanism, where the superconductivity is suppressed again when the magnetic field increases further.

While the exchange scattering in the Pb-Ce alloy films strongly suppresses superconductivity, it has almost no effect on the normal-state resistance. The exchange scattering time $\tau_s = \nu_s^{-1}$ (1.8 ps for F2) is 3 orders of magnitude longer than the transport scattering time τ_t , which can be estimated from R_N . Therefore, the Kondo effect [22] cannot be the main cause of the logarithmic T dependence shown in Fig. 1(d), which may be attributed to the weak localization effect in disordered two-dimensional systems [23].

The exchange coupling between a localized moment and conduction electrons is much stronger for 3d impurities than for 4f impurities. Although a small amount of Mn or Cr strongly suppresses the superconductivity of ultrathin Pb films, we did not observe the enhancement of T_c by H_{\parallel} when we deposited Mn or Cr directly onto the Pb film. This can be attributed to the formation of the Kondo singlet state [9], which was not taken into account in the KF theory. The Kondo temperature T_K , below which this state exists, depends exponentially on the exchange coupling constant J and can have a wide range of values. For $T_K \gg T_{c0}$, the pair-breaking effect of the localized moment vanishes and instead T_c is suppressed by an effective repulsive interaction between Cooper-pair electrons through the virtual polarization of the Kondo singlet state [24, 25]. In this regime, the suppression rate of T_c with magnetic impurities increases as T_K decreases. For $T_K \ll T_{c0}$, on the other hand, T_c is suppressed by the unscreened moment and the suppression rate is proportional to J^2 . We believe that the Pb-Ce films are in this regime since the H_{\parallel} dependence of T_c is successfully explained in terms of the KF theory. As schematically illustrated in Fig. 3(a), the suppression rate is expected to have a maximum as a function of T_K or $|J|$ [24].

To reduce the exchange coupling between the localized moment and conduction electrons, a 0.3 nm layer of Au was used to cover an ultrathin Pb film ($d = 1.1$ nm) before Mn deposition. Figure 3(b) shows the T dependence of R_{sq} at $H = 0$ for different densities n_{Mn} of Mn adatoms. The suppression rate is 2 orders of magnitude greater than that for Ce deposition [13] and superconductivity is fully suppressed for $n_{\text{Mn}} = 0.06 \text{ nm}^{-2}$ (≈ 0.006 monolayer). In Fig. 3(c), the H_{\parallel} -induced change in T_c is shown. Besides the negative quadratic H_{\parallel} dependence arising from PE, a small enhancement of T_c is observed after Mn deposition. Since PE is expected to depend

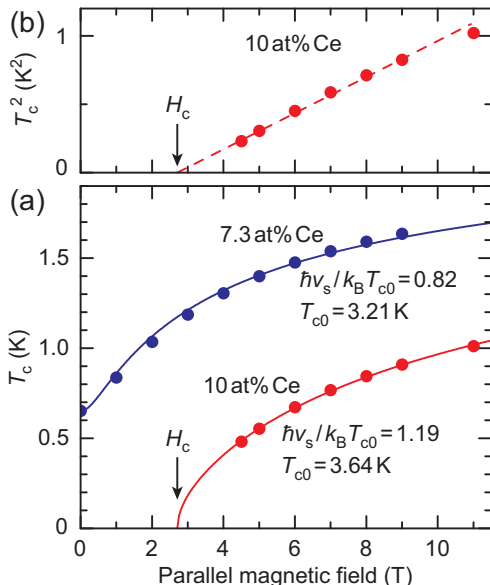


FIG. 2. Field-temperature phase diagram for Pb-Ce alloy films. (a) Circles are the H_{\parallel} dependence of T_c for F1 (blue) and F2 (red). Solid curves are calculations according to Ref. [8] with $S = 1/2$. (b) Square of T_c for F2.

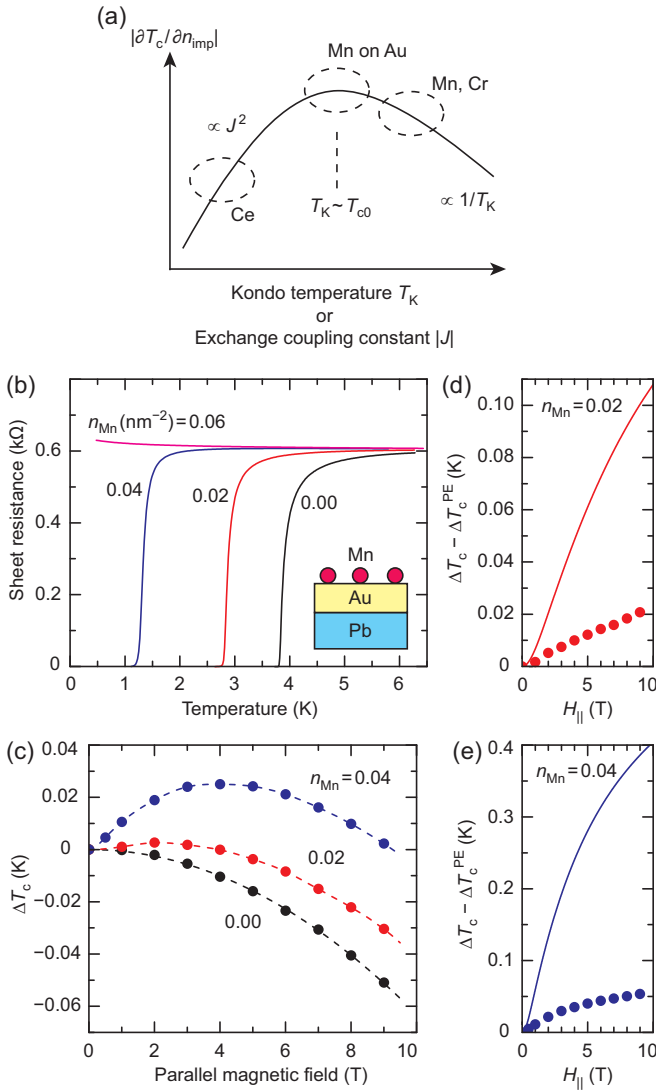


FIG. 3. Superconductivity of a Au/Pb film with Mn adatoms. (a) Schematic dependence of the suppression rate of T_c per magnetic impurity concentration on T_K (or $|J|$). (b) T dependence of R_{sq} of a Au/Pb film at $H = 0$ with varying n_{Mn} . (c) H_{\parallel} -induced change in T_c (ΔT_c) for different n_{Mn} . (d), (e) H_{\parallel} dependence of ΔT_c after subtracting PE. Solid curves are calculations based on Ref. [8].

only on τ_t for strong Rashba splitting [26], it can be estimated from the data for $n_{\text{Mn}} = 0$. After subtracting PE, the results for $n_{\text{Mn}} = 0.02$ and 0.04 nm^{-2} are plotted in Figs. 3(d) and 3(e), respectively. The solid curves are calculated based on the KF theory using $S = 5/2$ and $T_{c0} = 3.90 \text{ K}$ obtained from T_c for $n_{\text{Mn}} = 0$. The experimental enhancement of T_c is several times smaller than the calculation. This seems reasonable if the film is in the regime of $T_K \sim T_{c0}$, where the localized moment is partially screened by conduction electrons. In recent years, there has been a great interest in the Kondo screening of surface-adsorbed magnetic atoms and molecules [27–32],

partly due to their potential applications in nanoscale spintronic devices. It has been demonstrated here that the study of the H_{\parallel} dependence of T_c can provide valuable information on the degree of Kondo screening.

In conclusion, we observed a H_{\parallel} -induced superconducting quantum phase transition in a Pb-Ce(10 at%) alloy film. The H_{\parallel} dependence of T_c is well reproduced by the calculation based on a recent theory by Kharitonov and Feigelman [8], who considered the reduction of the exchange scattering rate in magnetic fields. This is in contrast to previously reported magnetic-field-induced superconductors [14–17], which are attributed to the Jaccarino-Peter mechanism [19]. While the formation of the Kondo singlet state [9] is not taken into account in the KF theory, it becomes important for $3d$ impurities. We found that the degree of Kondo screening of Mn adatoms can be reduced by capping the Pb film with a Au layer, and observed the positive H_{\parallel} dependence of T_c .

This work was supported by JSPS KAKENHI Grants No. JP26287072 and No. JP16H03998.

- [1] H. Kamerlingh Onnes, Proc. K. Ned. Akad. Wet. **16**, 987 (1914).
- [2] A. M. Clogston, Phys. Rev. Lett. **9**, 266 (1962).
- [3] B. S. Chandrasekhar, Appl. Phys. Lett. **1**, 7 (1962).
- [4] T. Sekihara, R. Masutomi, and T. Okamoto, Phys. Rev. Lett. **111**, 057005 (2013).
- [5] E. I. Rashba, Sov. Phys. Solid State **2**, 1109 (1960).
- [6] Yu. A. Bychkov and E. I. Rashba, JETP Lett. **39**, 78 (1984).
- [7] T. Sekihara, T. Miyake, R. Masutomi, and T. Okamoto, J. Phys. Soc. Jpn. **84**, 064710 (2015).
- [8] M. Yu. Kharitonov and M. V. Feigelman, JETP Lett. **82**, 421 (2005).
- [9] K. G. Wilson, Rev. Mod. Phys. **47**, 773 (1975).
- [10] T. Okamoto, T. Mochizuki, M. Minowa, K. Komatsuzaki, and R. Masutomi, J. Appl. Phys. **109**, 102416 (2011).
- [11] R. Masutomi and T. Okamoto, Appl. Phys. Lett. **106**, 251602 (2015).
- [12] See Supplemental Material for the calibration data on the magnetoresistance effect of the RuO $_2$ resistance thermometer (Scientific Instruments RO-600).
- [13] See Supplemental Material for the data on a 0.65 nm thick Pb film covered with Ce. The H_{\parallel} dependence of T_c is also shown.
- [14] H. W. Meul, C. Rossel, M. Decroux, Ø. Fischer, G. Remenyi, and A. Briggs, Phys. Rev. Lett. **53**, 497 (1984).
- [15] C. L. Lin, J. Teter, J. E. Crow, T. Mihalisin, J. Brooks, A. I. Abou-Aly, and G. R. Stewart, Phys. Rev. Lett. **54**, 2541 (1985).
- [16] S. Uji, H. Shinagawa, T. Terashima, T. Yakabe, Y. Terai, M. Tokumoto, A. Kobayashi, H. Tanaka, and H. Kobayashi, Nature (London) **410**, 908 (2001).
- [17] T. Konoike, S. Uji, T. Terashima, M. Nishimura, S. Yasuzuka, K. Enomoto, H. Fujiwara, B. Zhang, and H. Kobayashi, Phys. Rev. B **70**, 094514 (2004).
- [18] F. Lévy, I. Sheikin, B. Grenier, and A. D. Huxley, Science **309**, 1343 (2005).

- [19] V. Jaccarino and M. Peter, *Phys. Rev. Lett.* **9**, 290 (1962).
- [20] H. J. Gardner, A. Kumar, L. Yu, P. Xiong, M. P. Warusawithana, L. Wang, O. Vafek, and D. G. Schlom, *Nat. Phys.* **7**, 895 (2011).
- [21] A. A. Abrikosov and L. P. Gor'kov, *Sov. Phys. JETP* **12**, 1243 (1961).
- [22] J. Kondo, *Prog. Theor. Phys.* **32**, 37 (1964).
- [23] P. A. Lee and T. V. Ramakrishnan, *Rev. Mod. Phys.* **57**, 287 (1985).
- [24] T. Matsuura, S. Ichinose, and Y. Nagaoka, *Prog. Theor. Phys.* **57**, 713 (1977).
- [25] A. Sakurai, *Phys. Rev. B* **17**, 1195 (1978).
- [26] The coefficient for the negative quadratic H_{\parallel} dependence of T_c arising from PE is proportional to the effective spin-orbit scattering time, which can be replaced by τ_t when the spin precession frequency in the Rashba field is high enough [7].
- [27] J. Li, W.-D. Schneider, R. Berndt, and B. Delley, *Phys. Rev. Lett.* **80**, 2893 (1998).
- [28] V. Madhavan, W. Chen, T. Jamneala, M. F. Crommie, and N. S. Wingreen, *Science* **280**, 567 (1998).
- [29] L. Bogani and W. Wernsdorfer, *Nat. Mater.* **7**, 179 (2008).
- [30] K. J. Franke, G. Schulze, and J. I. Pascual, *Science* **332**, 940 (2011).
- [31] J. L. Zhang, J. Q. Zhong, J. D. Lin, W. P. Hu, K. Wu, G. Q. Xu, A. T. S. Wee, and W. Chen, *Chem. Soc. Rev.* **44**, 2998 (2015).
- [32] Z. Huang, Y. Zhang, Y. He, H. Song, C. Yin, and K. Wu, *Chem. Soc. Rev.* **46**, 1955 (2017).

SUPPLEMENTAL MATERIAL

Magnetoresistance effect of the RuO resistance thermometer

The RuO₂ resistance thermometer (RO-600) was manufactured by Scientific Instruments (SI), Inc., which offers a simple linear formula for a positive magnetoresistance. It allows the correction of any apparent temperature, measured in a magnetic field of up to 16 T, to the actual temperature with an error of less than $\pm 1.6\%$ for a broad temperature range of 0.036 to 4.2 K. To obtain better accuracy, we performed a systematic calibration up to 14 T using the vapor pressure of the liquid ³He or ⁴He. Our measurements reveal small T dependence while the variation is almost within the error bars for the SI's formula.

Pb film covered with Ce adatoms

As mentioned in the main text, we have performed transport measurements also on a 0.65 nm thick Pb film covered with Ce adatoms. Figure 5 shows the T dependence of the sheet resistance R_{sq} at $H = 0$ for different densities of Ce adatoms, $n_{Ce} = 0, 1.9, 3.7, 5.6, 7.4 \text{ nm}^{-2}$. Since $n_{Ce} = 7.4 \text{ nm}^{-2}$ is comparable with the planar densities of the bulk Ce(111) plane (8.7 nm^{-2}) and the bulk Pb(111) plane (9.4 nm^{-2}), it corresponds to a coverage near one monolayer. The superconducting transition shifts to lower temperatures with increasing n_{Ce} . As in the case of the Pb-Ce alloy films, it can be attributed to the exchange scattering of conduction electrons. In Fig. 6, T_c is shown as a function of H_{\parallel} . The enhancement

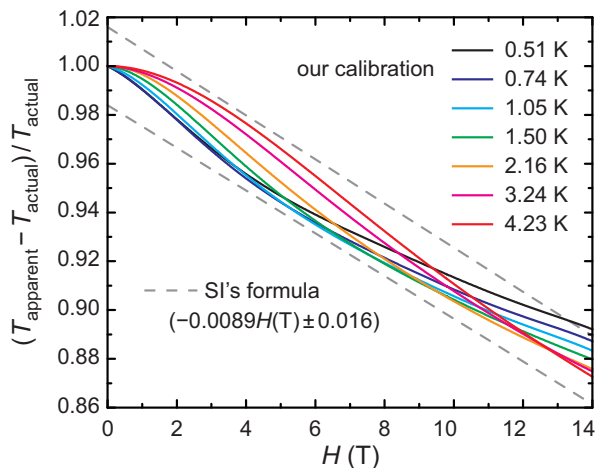


FIG. 4. Deviation of the apparent temperature indicated by a RO-600 thermometer from the actual temperature.

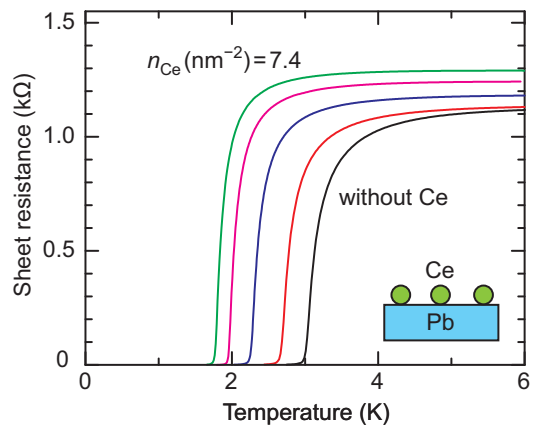


FIG. 5. Temperature dependence of the sheet resistance of a 0.65 nm thick Pb film at $H = 0$ for different Ce coverages.

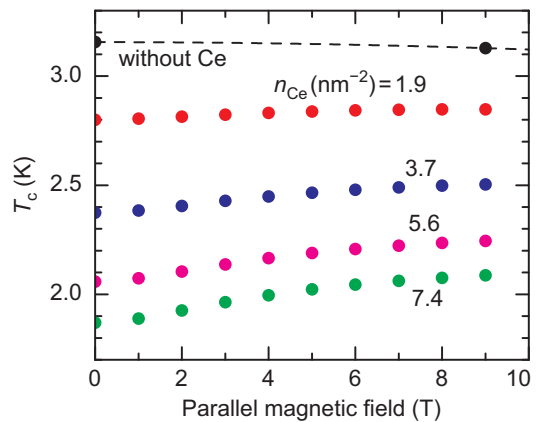


FIG. 6. Parallel magnetic field dependence of the superconducting transition temperature of a 0.65 nm thick Pb film for different Ce coverages.

of T_c by H_{\parallel} is observed after Ce deposition. It increases with increasing n_{Ce} while it is smaller than that observed in the Pb-Ce alloy films (see Fig. 2(a) of the main text).

Au/Pb film with Mn adatoms

The T dependence of R_{sq} of a Au/Pb film with Mn adatoms at $H = 0$ has been shown in Fig. 3(b) of the main text. In Fig. 7, H_{\parallel} induced shifts are presented. Before Mn deposition, the superconducting transition shifts to lower temperature with increasing H_{\parallel} . After Mn deposition, on the other hand, it shifts to higher temperature as H_{\parallel} increases from 0 to 4 T. As described in the main text, the data were carefully taken under thermal equilibrium with a RuO₂ resistance thermometer calibrated in magnetic fields. While T_c was defined as the temperature at which R_{sq} becomes $0.5R_N$, the H_{\parallel} induced change ΔT_c does not significantly depend on the

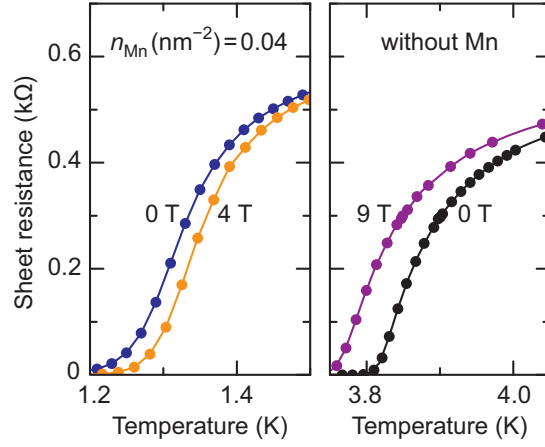


FIG. 7. Parallel-magnetic-field-induced shift in the superconducting transition in a Au/Pb film with and without Mn adatoms.

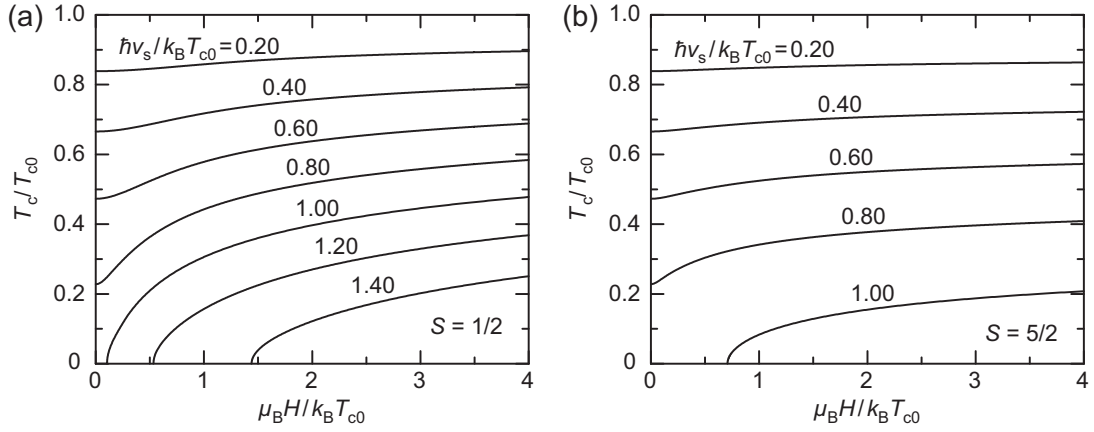


FIG. 8. H - T phase diagram based on the theory by Kharitonov and Feigelman. Results for different exchange scattering rates are shown for the case without OE and PE. (a) $S = 1/2$. (b) $S = 5/2$.

criterion resistance value. The H_{\parallel} dependence of ΔT_c was shown in Fig. 3(c) of the main text.

Calculations based on the theory by Kharitonov and Feigelman

In the presence of the exchange scattering, T_c at $H = 0$ is determined from the equation

$$\ln\left(\frac{T_c}{T_{c0}}\right) + \psi\left(\frac{1}{2} + \frac{\hbar\nu_s}{2\pi k_B T_c}\right) - \psi\left(\frac{1}{2}\right) = 0.$$

Here, T_{c0} is the transition temperature in the absence of exchange scattering, $\psi(x)$ is the digamma function, and ν_s is the exchange scattering rate at $H = 0$. This equa-

tion is equivalent to Eq. (1) in Ref. [8]. As ν_s increases, T_c monotonically decreases from T_{c0} and becomes zero for the critical scattering rate $\nu_s^* = \pi T_{c0}/2e^\gamma = 0.882T_{c0}$, where $\gamma = 0.577$ is the Euler's constant. The scattering rate can be represented as the sum of the spin-flip scattering rate and the rate of scattering without spin flip. When H increases from zero to infinity, the former decreases from $2\nu_s/3$ to zero while the latter increases from $\nu_s/3$ to $\nu_s S/(S+1)$. Thus, the total scattering rate decreases from ν_s to $\nu_s S/(S+1)$. For $\nu_s^* < \nu_s < \nu_s^*(S+1)/S$, if OE and PE are absent, H induces a superconducting quantum phase transition.

In finite magnetic fields, T_c is calculated numerically using Eqs. (4)-(6) and (9) in Ref. 1. The results for different S and ν_s are shown in Fig. 8. The H dependence of T_c is stronger for $S = 1/2$ (Ce) than for $S = 5/2$ (Mn).